ELSEVIER

Journal of Organometallic Chemistry 508 (1996) 129–136

Journal of Organometallic Chemistry

^{55}Mn and ^{187}Re NQR spectral studies of modulation effects of mutual motions of electrons and atomic nuclei in cyclopentadienyl tricarbonyl manganese and rhenium complexes

G.K. Semin *, S.I. Kuznetsov, E.V. Bryukhova, T.L. Khotsyanova

Institute of Organo-Element Compounds, Academy of Sciences of Russia, 28 Vavilov Street, Moscow 117813, Russia

Received 3 May 1995

Abstract

The ^{55}Mn and ^{187}Re NQR spectral parameters for cyclopentadienyl tricarbonyl complexes of these metals at 77 K are presented. An analytical dependence between e^2Qq_{zz} and η has been shown to exist. Such dependence may be associated with slow mutual electron–nuclear motions in these complexes.

Keywords: Manganese; Rhenium; Carbonyls; Nuclear Quadrupole Resonance; Electron–nuclear motions

1. Introduction

The mechanism of bond formation between the cyclopentadienyl ring and a metal atom is a problem that has not yet been resolved. The basic reason for this situation is that methods usually employed for studying the problem are incapable of elucidating the role of dynamic effects during such types of bond formation. In addition, if several configurational distributions exist for the electron density in a coordination complex or molecular system, and, if dynamic transitions occur between these configurational states due to the electron tunnelling, splitting the electron energy levels will result; such splittings are usually called tunnel or inversion splittings. They are caused by phase changes in the wave packets upon tunnelling from one energy well to another on the potential energy curve [1] and lead to additional differences in the electron distribution configurations. The above differences may be observed (or remain unnoticed) when the mutual positions of the atomic nuclei in a molecule or complex change and depend on the ratio of the lifetimes of the nuclei in the configurational states as well as on the ratio, τ, of the total electron-transfer times for tunnelling to the characteristic times for the motion of atomic nuclei. An essential feature of this model is that changes occur in the ratio of the characteristic times for electron motions to those for the motion of atomic nuclei.

The characteristic times for electron motions are usually assumed to be some 5–10 orders of magnitude less than those for the motions of atomic nuclei. This assumption provides the basis for the well-known Born–Oppenheimer limitation [2], according to which quantum interactions between electrons and atomic nuclei can be neglected because of enormous difference between the characteristic times for their motions.

However, the probability of passing through a potential barrier upon electron tunnelling is 10^{-5} to 10^{-10} in typical cases [1], resulting in an increase in the correlation time τ for total electron transfer from one potential well to another one. The only exception to this situation is resonance tunnelling [1]. On the basis of the close values of the above estimates, it is possible to assume that times for total electron transfer upon tunnelling might, in several cases, be close to or coincide with the characteristic times for the motion of atomic nuclei. This means that the Born–Oppenheimer limitation [2] will no longer be valid in this region, and that hybrid electron–nuclear states will be generated [3].

Theoretical studies of the effect described above

* Corresponding author.

SSDI 0022-328X(95)05794-3

Table 1
^{55}Mn NQR spectral parameters at 77 K in the $(CO)_3MnC_5H_{5-n}R_n$ series

No.	R_n	e^2Qq_{zz} (MHz)	η(%)	No.	R_n	e^2Qq_{zz} (MHz)	η(%)
1	$C_{17}H_{21}OSi$ [a]	64.670	(−)10.6	24	$Sn(n-C_4H_9)_3$	63.58	2.0
2	C_2H_5	64.708	(−)9.1	25	CH=NOH	62.909	3.5
3	$(CH_2I)_2$	64.689	(−)7.45	26	HgCl phase 1	62.30	4.8
4	CH_2Cl	64.950	(−)5.1	27		65.41	10.2
5	CH_3	64.860	(−)4.4	28	HgCl phase 2	64.20	(−)10.3
6	H	65.20	1.9	29		65.17	2.0
7	SO_3Na	65.81	2.9	30	HgBr	63.99	(−)3.2
8	$(CH_3)_3$	65.919	3.35	31		65.97	9.6
9	I	67.014	5.1	32	HgI	63.199	3.45
10	Br	67.44	5.3	33		65.139	12.6
11	Cl	67.65	5.4	34	$(CO)_3MnC_5H_4Hg$	63.525	9.9
12	$(CH_3)_4$	68.782	5.7	35		64.070	(−)3.0
13	$(CH_3)_5$	69.337	5.8	36	$COOCH_3$	61.200	5.6
14	$(C_2H_5)_5$	71.152	5.95	37	$COCH_3$	61.630	6.8
15	Cl_5	78.922	6.2	38	COH	61.378	9.0
16		77.388	7.2	39	COCl	59.940	10.3
17	SO_2CH_3	63.424	6.63	40	$COCH_2Br$	60.700	10.6
18	SO_2NH_2	63.56	6.64	41	$COCH_2Cl$	60.740	10.65
19	$SO_2C_2H_5$	64.396	6.70	42	COC_6H_5	62.422	12.4
20	$(CH_2Cl)_2$	65.234	6.76	43	$COCF_3$	59.350	13.9
21	$(CH_2Br)_2$	65.099	6.75	44	$C_6H_9O_3S$ [b]	62.25	7.5
22	SO_2Cl	61.74	8.3	45	COOH	62.27	0
23	$Sn(C_6H_5)_3$	63.90	(−)3.5				

[a] $C(OH)(C_6H_5)\ CH_2C_6H_4Si(CH_3)_3$ – 4,4′.
[b] $C(O)CH_2CHCH_2CH_2SO_2CH_2$.

have encountered computing problems which were difficult to overcome because the adiabatic approach is no longer valid. This is why experimental evidence for this process becomes so important.

Nuclear quadrupole resonance (NQR) is associated with the existence of gradient electric fields on atomic nuclei. The method is the most appropriate for studying the problem because of its high accuracy and, hence, of its high level of information. An important point is that NQR frequencies are proportional to the second derivative of the electrostatic potential, whose changes are much more pronounced than those of the function itself.

The main spectral characteristics obtained from NQR spectra are: the quadrupole coupling constant (QCC), i.e. e^2Qq_{zz}, where eQ is the electric quadrupole moment of the atomic nucleus (the nuclear constant), eq_{zz} is the maximum diagonal component of the electric field gradient (EFG) tensor at the atomic nucleus, ($eq_{zz} = \partial^2U/\partial z^2$ is the second derivative of the electrostatic potential at the atomic nucleus), and the EFG asymmetry parameter

$$\eta = |(q_{xx} - q_{yy})/q_{zz}| \quad (1)$$

where q_{xx}, q_{yy}, q_{zz} are the principal diagonal components of the EFG tensor

$$|q_{xx}| < |q_{yy}| < |q_{zz}| \quad (2)$$

In accordance with the Laplace condition, at the nucleus

$$q_{xx} + q_{yy} + q_{zz} = 0 \quad (3)$$

Changes in the QCC and η with temperature arise from periodic and fast changes in the mutual orientation of the EFG tensor and the nuclear quadrupole moment tensor during the free thermal vibrations of the molecules (in the limiting case these are hindered reorientations).

Another source of temperature changes in the QCC and η is modulation of the EFG caused by thermal translational motions of neighbouring molecules. It is the mechanism of EFG averaging by the comparatively slow mutual intramolecular motions of electrons and atomic nuclei which has not been considered earlier by other authors.

In the present work an attempt has been made to consider changes in the EFG at a fixed temperature (77 K) caused by configurational instability due to interconfigurational electron tunnelling. With this aim in mind, we have chosen the molecular system $(CO)_3Mn(Re)C_5H_{5-n}R_n$, since the resonant atom, ^{55}Mn(^{187}Re), is in the centre of the molecule and most affected by the configurational electron instability.

2. Experimental details

All measurements of ^{55}Mn and ^{187}Re NQR spectra were carried out at 77 K on the NQR spectrometer/relaxometer ISSh-2-13 developed and produced by SKB-IRE AN SSSR [4].

All known quadrupole coupling constants (e^2Qq_{zz})

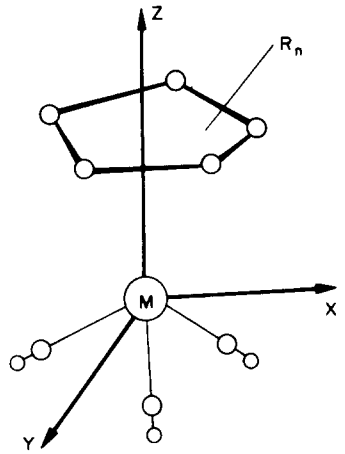

Fig. 1. Position of the EFG axes for molecules in the $(CO)_3MnC_5H_{5-n}R_n$ series.

and asymmetry parameters (η) in the series $(CO)_3MnC_5H_{5-n}R_n$ (Nos. 1–35) and $(CO)_3MnC_5H_4COX$ (Nos. 36–45) [5] are listed in Table 1. Apart from literature data, some of the listed spectra were studied for the first time, some were refined. As is shown by the spectra for compounds with $R_n = Cl_5$, HgBr, HgI and $HgH_4C_5Mn(CO)_3$, their molecules occupy two crystallographically non-equivalent positions. For $(CO)_3MnC_5H_4HgCl$ both crystalline phases were studied (at 77 K). In our subsequent calculations, data for different crystallographically non-equivalent positions were not averaged, but used separately for each position. Hence we used the common numbering given in Table 1. Formal changes in the asymmetry parameters signs indicating changes in the positions of x- and y-components will be explained below in the text.

Table 2 lists the numerical values of e^2Qq_{zz} and η from the ^{187}Re NQR spectra of the $(CO)_3ReC_5H_{5-n}R_n$ series [5]. The meaning of the column with the τ values will be explained below in the text.

3. Results and discussion

As can be seen from the scheme in Fig. 1, the EFG on the ^{55}Mn nucleus as observed by the NQR method is the difference between the contributions to the EFG from different parts of the π-cyclopentadienyl tricarbonyl manganese molecule, i.e. (1) from the three CO groups and (2) from the cyclopentadienyl ring and its substituents.

The charge separation between the manganese atom and the cyclopentadienyl ligand increases upon the addition of electron-donor substituents to the cyclopentadienyl ring, which results in an increase in the quadrupole coupling constant e^2Qq_{zz} for ^{55}Mn. In contrast, the addition of electron-acceptor substituents decreases the value of e^2Qq_{zz} on the manganese atom (see Tables 1 and 2).

The redistribution of charge leads to a change in the characteristics of the interconfigurational transitions as well as in e^2Qq_{zz} and η. The process of searching for a minimum in the energy system involving such configurational transitions is accompanied by mutually related fluctuations in the energy and in the shape of the electron distribution, whose measure in NQR spectroscopy is provided by the asymmetry parameters. By comparing the changes in e^2Qq_{zz} and η, it is possible to observe the dynamics of these transitions. In this case, changes in the dimensionless quantity η will characterize changes in the energy characteristics of the electron configuration, while changes in e^2Qq_{zz} define the intrabonding charge distribution in $(CO)_3MnC_5H_{5-n}R_n$, including the 'recharge' process associated with the change in the direction of the 'induced' bond dipole [7].

For convenience in analyzing experimental data, we can divide the observed EFG tensor with components e^2Qq_{xx}, e^2qQ_{yy}, e^2Qq_{zz} and $\eta = |(q_{xx} - q_{xx})/q_{zz}|$ [Eq. (1)] into two parts: the unchanged EFG tensor (at a given temperature) with components eqQ_{xx0}, eqQ_{yy0}, eQq_{zz0} and

$$\eta_0 = |(q_{xx0} - q_{yy0})/q_{zz0}| \quad (4)$$

and the 'induced' EFG tensor with components $(e^2Qq_{xx} - e^2Qq_{xx0})$, $(e^2Qq_{yy} - e^2Qq_{yy0})$, $(e^2Qq_{zz} - e^2Qq_{zz0})$ and

$$\eta_{ind} = |[(q_{xx} - q_{xx0}) - (q_{yy} - q_{yy0})]/(q_{zz} - q_{zz0})| \quad (5)$$

Table 2
^{187}Re NQR spectral parameters at 77 K in the $(CO)_3ReC_5H_{5-n}R_n$ series

No.	R_n	e^2Qq_{zz} (MHz)	η(%)	τ (10^{-14}s)	No.	R_n	e^2Qq_{zz} (MHz)	η(%)	τ (10^{-14}s)
1	$(CH_3)_5$	721.83	(−)23.3	46.41	8	$Sn(C_6H_5)_3$	539.10	(−)15.0	26.73
2	$(CH_3)_4$	691.03	(−)16.3	28.65	9	$COCH_3$	548.47	30.5	39.45
3	$(CH_3)_3$	652.74	(−)3.9	15.61	10	COOH	528.44	23.4	
4	$(CH_3)_2$	633.27	6.1	8.79	11	$COOCH_3$	496.61	8.95	
5	CH_3	610.53	17.1	1.89	12	COCl	478.25	39.1	4.70
6	I	601.90	17.1	1.89	13	COC_6H_5	464.66	41.8	1.97
7	H	586.64	8.7	7.15					

From Eqs. (1), (4) and (5) under condition (3) for all three sets of EFG components, we can derive an equation relating e^2Qq_{zz}, η, η_{ind}, η_0 and e^2Qq_{zz0}, i.e.

$$\frac{e^2Qq_{zz}}{e^2Qq_{zz0}} = \frac{\eta_0 - \eta_{ind}}{\eta - \eta_{ind}} \tag{6}$$

If in a series of compounds of the same type the difference between two transversal EFG components $(e^2Qq_{xx} - e^2Qq_{yy})$ depends on the change in the longitudinal component (e^2Qq_{zz}), i.e. $(e^2Qq_{xx} - e^2Qq_{yy}) = f(e^2Qq_{zz})$, the increment of the function $\eta(e^2Qq_{zz})$ and of the argument (e^2Qq_{zz}) must be related by an approximate equality $\delta\eta = \delta q_{zz} \cdot d\eta/dq_{zz}$, as is known. Taking into account that according to Eq. (1) the signs of q_{zz} and $d\eta/dq_{zz}$ are different, at $\delta\eta = (\eta - \eta_0)$ and $\delta q_{zz} = (q_{zz} - q_{zz0})$ we get

$$\frac{d\eta}{\eta_0 - \eta} = \frac{dq_{zz}}{q_{zz} - q_{zz0}} \tag{7}$$

After solving Eq. (7) as a differential equation with separated variables, simple transformations lead to the relationship:

$$(e^2Qq_{zz} - e^2Qq_{zz0})(\eta_0 - \eta) = B \cdot \delta \tag{8}$$

where B is a constant for a given series and $\delta = \pm 1$ [6]. From Eqs. (6) and (8) one can see that

$$\eta_{ind} = \eta - \delta \cdot \frac{e^2Qq_{zz0}}{B}(\eta_0 - \eta)^2 \tag{9}$$

In fact, Eq. (8) describes the picture observed experimentally quite well [6,7] except in the close vicinity of η_0.

It is interesting to note that the form of Eq. (8) coincides with that of the $e^2Qq_{zz}(I)$ dependence for $Cl_5Sb \cdot L_0$ complexes [7], where L_0 is an oxygen-containing ligand, with I being the ionization potential for the lone pair electron of the oxygen atom. This confirms the above-mentioned considerations that energy changes and fluctuations must result in configurations whose measure are changes in η, i.e. $\delta I \sim \delta\eta$ [7].

Departures from dependence (8) in the vicinity of η_0 can be understood, if it is assumed the EFG fluctuations occur with an average modulation depth $\Delta\eta$ in the vicinity of (η_0, e^2Qq_{zz0}). If such EFG fluctuations are of a stochastic nature due to the multiplicity of the vibration processes, one can use the basic relationships of the theory of stochastic dynamics of non-linear vibration systems [8]. This theory predicts the appearance of a nearly rectangular spectrum for comparatively low frequency vibrations. In this case one can carry out a simple integrated averaging of Eq. (8) to take account of the mutual modulation motions of electrons and atomic nuclei when computing the observed e^2Qq_{zz} values

$$e^2Qq_{zz} = \frac{1}{2\Delta\eta}\int_{\eta-\Delta\eta}^{\eta+\Delta\eta}\left[e^2Qq_{zz0} + \frac{B \cdot \delta}{(\eta_0 - \eta)}\right]d\eta$$

$$= e^2Qq_{zz0} + \frac{B \cdot \delta}{2\Delta\eta}\ln\left|\frac{\eta - (\eta_0 + \Delta\eta)}{\eta - (\eta_0 - \Delta\eta)}\right| \tag{10}$$

or in the interval $(\eta_0 \pm \Delta\eta)$

$$\left|\frac{\eta - \eta_0}{\Delta\eta}\right| = \text{th}\left|\frac{\Delta\eta}{B}(e^2Qq_{zz} - e^2Qq_{zz0})\right| \tag{11}$$

At $|(\eta - \eta_0)/\Delta\eta| = 2.5$–$3$ and above, the descriptive power of Eqs. (8) and (10) is almost equal.

A similar averaging can be obtained for η_{ind} using Eq. (9)

$$\bar{\eta}_{ind} = \frac{1}{2\Delta\eta}\int_{\eta-\Delta\eta}^{\eta+\Delta\eta}\left[\eta - \delta \cdot \frac{e^2Qq_{zz0}}{B}(\eta - \eta_0)^2\right]d\eta$$

$$= \eta - \delta \cdot \frac{e^2Qq_{zz0}}{B}\left[(\eta - \eta_0)^2 + \frac{\Delta\eta^2}{3}\right] \tag{12}$$

3.1. Estimation of the total interconfigurational tunnel electron-transfer times (τ)

For a rough estimate of the total interconfigurational tunnel electron transfer, one can use the results reported in Ref. [9] where various aspects of the dipole instability have been considered. Let us consider two or more configurations of the electron distribution with different magnitudes and directions for their dipole moments undergoing the effect of local microscopic fields with the field strength ε. For a Boltzmann's distribution and $p_0\varepsilon \ll \delta E$, where p_0 is the absolute value of the dipole moment for an equilibrium configuration, and δE is the inversion (tunnel) splitting, the average dipole moment appears to be

$$\bar{P} = \frac{P_0^2\varepsilon}{3\delta E}\,\text{th}|\,\delta E/kT\,| \tag{13}$$

However, if the dipole generated in the case of the orientational polarization of 'hard' dipoles is written as

$$\bar{P}' = \frac{P_0^2\varepsilon}{3kT} \tag{14}$$

the $\bar{P}/\bar{P}'$ ratio will be

$$\frac{\bar{P}}{\bar{P}'} = \frac{kT}{\delta E}\,\text{th}\left|\frac{\delta E}{kT}\right| \tag{15}$$

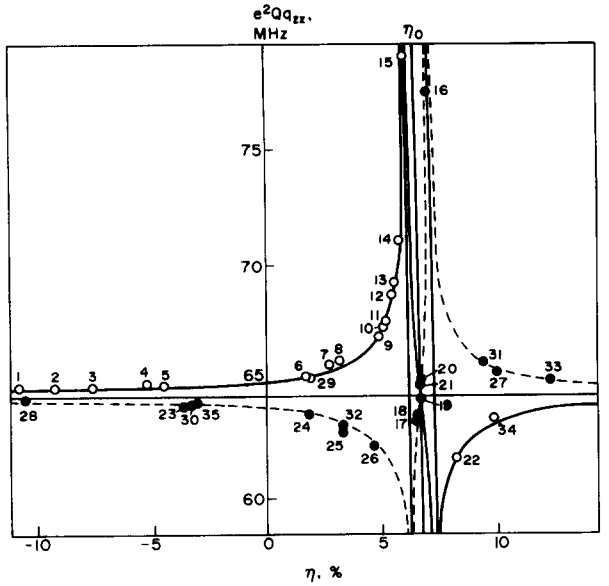

Fig. 2. Dependence of e^2Qq_{zz} on η for molecules in the $(CO)_3MnC_5H_{5-n}R_n$ series (see Nos. 1–35 in Table 1) as derived from Eq. (10): solid lines correspond to $\delta = +1$ (open points); dashed lines correspond to $\delta = -1$ (filled points).

Since the sources of changes in the asymmetry parameter η have the same origin, then setting

$$\bar{P}/\bar{P}' \sim (\eta - \eta_0)/\Delta\eta \tag{16}$$

and using expression (11) one can obtain an approximate equation

$$\left|\frac{\eta - \eta_0}{\Delta\eta}\right| = \frac{kT}{\delta E}\,\mathrm{th}\left|\frac{\delta E}{kT}\right| \tag{17}$$

Eq. (17) allows one to estimate δE at a fixed temperature using the parameters of Eq. (10) and experimental values for e^2Qq_{zz}. Values of τ and δE are known to be related [1] by a simple dependence

$$\tau = \pi\hbar/\delta E \tag{18}$$

Tables 2 and 4 list the τ-values for experimental points lying in the range $(\eta_0 \pm \Delta\eta)$. From a rough estimation it is seen that the τ-values generally lie in the interval 8×10^{-13} into 3×10^{-15} s, i.e. within the range of characteristic times for nuclear motions. The direction of decrease in τ is $\eta_0 \pm \Delta\eta \rightarrow \eta_0$ and hence points corresponding to $(\eta_0 \pm \Delta\eta)$ are associated with the appearance of a slow tunnelling effect, while the point at η_0 corresponds to the most rapid electron tunnelling (see Fig. 2).

In all cases τ is smaller than the NQR characteristic times (10^{-6}–10^{-9} s), i.e. the observed EFG values are always averaged. The only factor which changes is the efficiency of averaging by interconfigurational electron tunnelling.

3.2. Manganese-55 NQR data for $(CO)_3MnC_5H_{5-n}R_n$ at 77 K

We can use data from Table 1 for the $(CO)_3MnC_5H_{5-n}R_n$ series (Nos.1–35 in Table 1) and for the $(CO)_3MnC_5H_4COX$ series (Nos. 36–44 in Table 1) to check the validity of relation (10). Both sets of experimental data are described by Eq. (10) with a high degree of accuracy (see Table 3 and Figs. 2 and 3). When the parameters of Eq. (10) are used for molecules in the $(CO)_3MnC_5H_4COX$ series (Table 3, line 2), the origin of the resulting curve is shifted with respect to the corresponding curve for molecules in the $(CO)_3MnC_5H_{5-n}R_n$ series (Table 3, line 1) in such a way along the e^2Qq_{zz0} and η axes that e^2Qq_{zz0} (1)

Table 3
Parameters of Eq. (10) for the $(CO)_3MnC_5H_{5-n}R_n$ series (series 1) and the $(CO)_3MnC_5H_4COX$ series (series 2) (from ^{55}Mn NQR spectroscopy at 77 K) [a]

Series No.	No. in Table 1	e^2Qq_{zz0} (MHz)	B (MHz %)	η_0 (%)	$\Delta\eta$ (%)	$\pm\delta e^2Qq_{zz}$ (MHz)	n	r
1 = R_n	1–35	64.451	4.018	6.7055	0.5285	0.09	35	0.999
2 = COX	36–44	60.272	3.588	10.0245	1.9943	0.08	9	0.996

[a] Where n is the number of experimental points used in calculating the parameters of Eq. (10) and r is the correlation coefficient between the calculated values from Eq. (10) and the experimental e^2Qq_{zz} values.

Table 4
Values of τ in the interval $(\eta_0 \pm \Delta\eta)$ for the $(CO)_3MnC_5H_{5-n}R_n$ series [a]

No. in Table 1	$\tau(10^{-14}$s)	No. in Table 1	$\tau(10^{-14}$s)	No. in Table 1	$\tau(10^{-14}$s)
15	83.99	19	0.32	38	16.82
16	68.11	20	3.21	39	4.30
17	4.45	21	2.62	40	9.00
18	3.86			41	9.82

[a] Calculated via Eqs. (17) and (18).

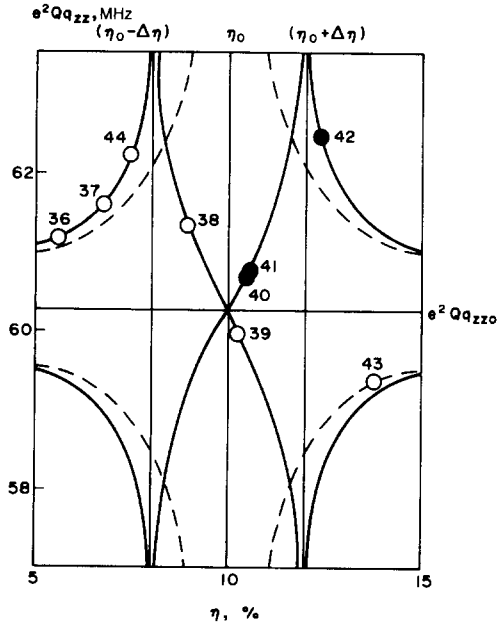

Fig. 3. The same dependence as in Fig. 2 for molecules in the $(CO)_3MnC_5H_4COX$ series (see Nos. 36–44 in Table 1). Solid lines relate to Eq. (10); dashed lines relate to Eq. (8). Notation the same as in Fig. 2.

$> e^2Qq_{zz}$ (2) and $\eta_0(1) < \eta_0(2)$. The specific nature of the effect of COX substituents has been described earlier [5].

One can see from Fig. 2 and Table 1 that most π-donor organic substituents and halogen atoms lie on the curve derived from Eq. (10) with $\delta = +1$. Organoelement and organometallic substituents, most of which are π-acceptors, lie on the branch of the curve derived from Eq. (10) with $\delta = -1$.

A graphic solution of Eq. (10) for molecules of the $(CO)_3MnC_5H_4COX$ series with $\delta = \pm 1$ is depicted by solid lines in Fig. 3 while that of Eq. (8) with $\delta = \pm 1$ is depicted by dashed lines.

The overlap between the experimental points demonstrates the comparative descriptive power of Eqs. (8) and (10) as well as differences between them [the only exception to Eq. (10) is point No. 45 (R = COOH), which might be due to the uncertainty caused by complex formation by water molecules during hydration].

A solution of Eq. (10) ($\delta = \pm 1$) using the coordinates e^2Qq_{zz} and e^2Qq_{ii}, where $i = x, y$, for molecules in the $(CO)_3MnC_5H_{5-n}R_n$ series (Nos. 1–35 in Table 1) is shown in Fig. 4. Open points correspond to $\delta = +1$ while filled points correspond to $\delta = -1$. The values of e^2Qq_{xx} and e^2Qq_{yy} were determined using Eqs. (1) and (3) with module values of η as expressed by:

$$e^2Qq_{xx} = -0.5(1-\eta)e^2Qq_{zz};$$

$$e^2Qq_{yy} = -0.5(1+\eta)e^2Qq_{zz} \qquad (19)$$

Intersection of the straight line corresponding to $\eta = 0$ by the curves $e^2Qq_{xx}(e^2Qq_{zz})$ and $e^2Qq_{yy}(e^2Qq_{zz})$ is clearly demonstrated in Fig. 4. It means that the X- and

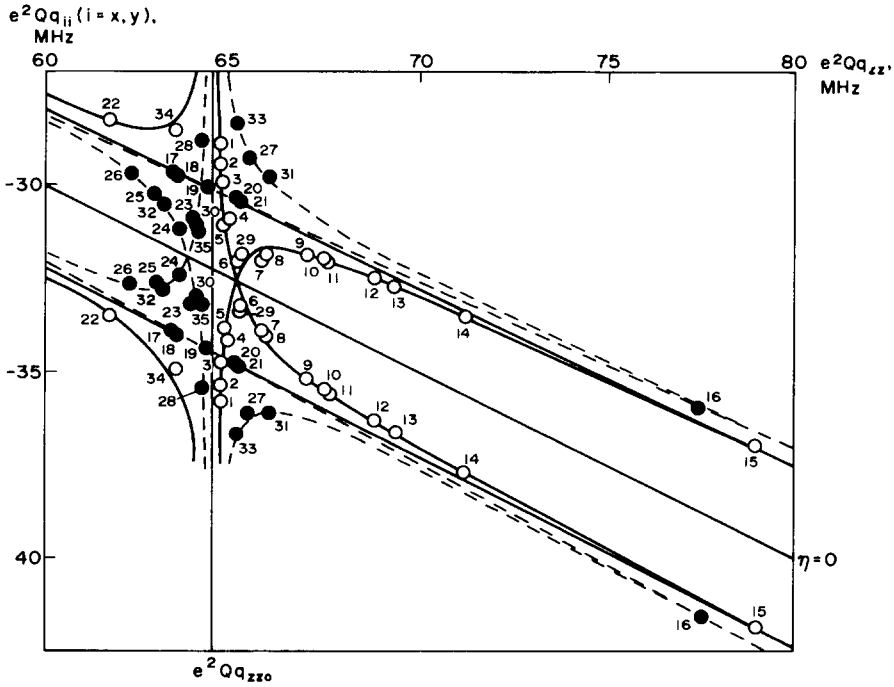

Fig. 4. Graphic solution of Eq. (10) for the $(CO)_3MnC_5H_{5-n}R_n$ series employing e^2Qq_{zz} and e^2Qq_{ii} coordinates, where $i = x, y$. Notation the same as in Fig. 2.

Table 5
Parameters of Eq. (10) for the $(CO)_3ReC_5H_{5-n}R_n$ series (series 1) and the $(CO)_3ReC_5H_4$ COX series (series 2) (from ^{187}Re NQR spectroscopy at 77 K) [a]

Series No.	No. in Table 2	e^2Qq_{zz0} (MHz)	B (MHz %)	η_0 (%)	$\Delta\eta$ (%)	$\pm\delta e^2Qq_{zz}$ (MHz)	n	r
$1 = R_n$	1–8	608.783	4185.888	20.117	49.755	2.0	8	0.999
2 = COX	9–13	468.889	834.343	41.002	12.595	0.3	5	0.999

[a] Where n is the number of the experimental points used in calculating the parameters of Eq. (10) and r is the correlation coefficient between the calculated values from Eq. (10) and the experimental e^2Qq_{zz} values.

Y-components in sequence expressed in Eq. (2) change places (for $\delta = +1$ such a point lies between No. 5 and No. 6, and for $\delta = -1$ between No. 24 and No. 30). The formal change in the sign of η is tantamount to a change in the e^2Qq_{xx} and e^2Qq_{yy} direction [10] (see Table 1, Fig. 2 and Eq. (10)).

From Figs. 2 and 3 it can be seen that several experimental points lie in the interval $(\eta_0 \pm \Delta\eta)$. Using relations (17) and (18), η_0 and $\Delta\eta$ values from Table 3, it is possible to estimate the correlation times for total electron transfer as a consequence of tunnel interconfigurational transitions [Eq. (18)] (see Table 4). In accordance with our estimates, τ-values computed from the experimental data lie in the interval 8.4×10^{-13} to 3×10^{-15} s, i.e. despite the fact that they are only rough estimates they are within the range of characteristic motion times for atomic nuclei (10^{-10}–10^{-14} s).

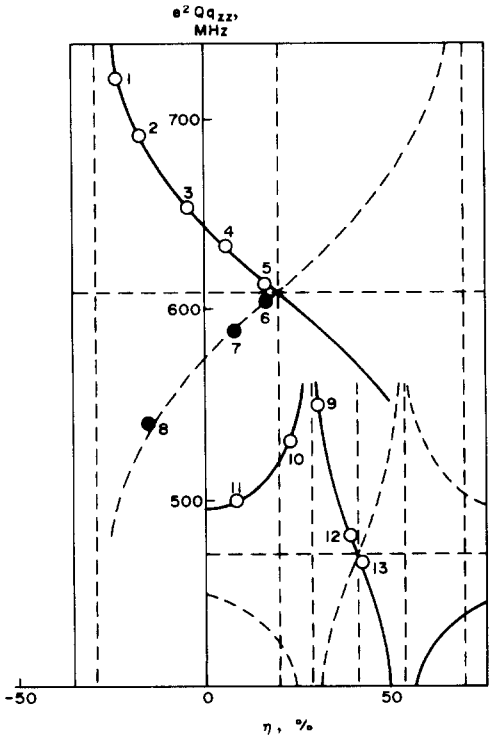

Fig. 5. Dependence of e^2Qq_{zz} on η for (a) molecules in the $(CO)_3ReC_5H_{5-n}R_n$ series (see Nos. 1–8 in Table 2) and (b) molecules in the $(CO)_3ReC_5H_4COX$ series (see Nos. 9–13 in Table 2).

3.3. Rhenium-187 NQR data for $(CO)_3ReC_5H_{5-n}R_n$ at 77 K

Further evidence for the reality of the processes described using the suggested model of interconfigurational tunnel transitions may be obtained from a comparison between the $\eta(e^2Qq_{zz})$ values for ^{187}Re at 77 K and those for manganese compounds similar to those in the $(CO)_3ReC_5H_{5-n}R_n$ series (see Table 2). Despite the much narrower experimental basis relative to the manganese analogues, it was possible to obtain parameters via Eq. (10) for both the $(CO)_3ReC_5H_{5-n}R_n$ series (Nos. 1–8) (series 1) and $(CO)_3ReC_5H_4COX$ series (Nos. 9–13) (series 2) (see Table 5 and Fig. 5). The relationships obtained appear to be: $\Delta\eta_{Mn}(1) \ll \Delta\eta_{Re}(1)$ and $\Delta\eta_{Mn}(2) \ll \Delta\eta_{Re}(2)$. The shift of relation (10) for both series is similar to that for the manganese analogues, with only the relationship $\Delta\eta_{Mn}(1) < \Delta\eta_{Mn}(2)$ changing while $\Delta\eta_{Re}(1) > \Delta\eta_{Re}(2)$ remains valid.

Estimates of τ-values for the experimental data in the interval $(\eta_0 \pm \Delta\eta)$ in the last column of Table 2 lie within the limits 5×10^{-13} to 2×10^{-14} s, i.e. also within the range of characteristic motion times for atomic nuclei.

4. Conclusions

From the highly descriptive power of Eq. (10) associated with estimates of electron motion times obtained from Eqs. (17) and (18), and the characteristic times of motion of atomic nuclei it is possible to demonstrate the existence of a real process, i.e. EFG averaging by comparatively slow mutual motions of electrons and atomic nuclei during tunnel interconfigurational transitions in $(CO)_3MC_5H_{5-n}R_n$ (M = Mn, Re) compounds.

The similarity between the theoretical curves derived from Eq. (10) (see Figs. 2, 3 and 5) and the dispersion curves suggests that the observed effect may be designate 'dispersion of electron nuclear motions' (DENM).

Consideration of DENM phenomena is important for understanding the nature of bonding of the π-cyclopentadienyl ring to a metal atom, since only via this phenomenon is it possible to understand the mechanism of the charge distribution in the so-called 'recharge' region.

It is that the development of low-frequency dynamics by electron systems in the DENM region will result in important changes in the reactivity and catalytic activity of compounds in the solid state as well as in anomalies in the electromagnetic properties of their crystals.

References

[1] E.O. Kane, in *Tunneling Phenomena in Solids*, Plenum Press, New York, 1969, pp. 9–24.
[2] M. Born and R. Oppenheimer, *Ann. Phys., 84* (1927) 457.
[3] B.S. Tsukerblat and M.I. Belinskii, *Magnetochemistry and Radiospectroscopy of Exchange Clusters*, Kiev, 1983, pp. 219–249 (in Russian).
[4] B.N. Pavlov, in *Pribory i oborudovanie dlya nauchnykh issledovaniy*, Moscow, 1983, pp. 6–15 (in Russian).
[5] G.K. Semin, T.A. Babushkina and G.G. Yakobson, *NQR in Chemistry*. John Wiley & Sons, New York/Toronto, 1975.
[6] G.K. Semin, S.I. Kuznetsov, E.V. Bryukhova and S.I. Gushin, *Abs. XIth Int. Symp. NQR Spectrosc.*, London, UK, 1991, p. 11:35; G.K. Semin, S.I. Kuznetsov, A.M. Raevsky and E.V. Bryukhova, *Z. Naturforsch., Teil A, 49* (1994) 630.
[7] G.K. Semin, *Abs. Xth Int. Symp. NQR Spectrosc.*, Takayama, Japan, 1989, v P27; *Abs. XIth Int. Symp. NQR Spectrosc.*, London, UK, 1991, p. 11:32.
[8] B.V. Chirikov, *Phys. Rep., 52* (1978) 263.
[9] I.B. Bersuker, *Teor. Eksp. Khim., 5* (1969) 293 (in Russian).
[10] G.K. Semin, S.I. Gushchin, E.V. Bryukhova et al., *Dokl. Akad. Nauk SSSR, 282* (1985) 1126 (in Russian).